Generic non-Fermi-liquid behavior of the resistivity in magnets with ferromagnetic, helical, or skyrmionic order

T. R. Kirkpatrick and D. Belitz

Phys. Rev. B **97**, 064411 — Published 20 February 2018

DOI: 10.1103/PhysRevB.97.064411

Generic non-Fermi-liquid behavior of the resistivity in magnets with ferromagnetic, helical, or skyrmionic order

T.R. Kirkpatrick[1] and D. Belitz[2]
[1] *Institute for Physical Science and Technology, University of Maryland, College Park, MD 20742*
[2] *Department of Physics, Institute of Theoretical Science, and Materials Science Institute, University of Oregon, Eugene, OR 97403*
(Dated: January 19, 2018)

The electrical resistivity of several relatively clean metallic ferromagnets, as well as the helimagnet MnSi, is commonly observed to exhibit non-Fermi-liquid behavior at low temperatures. This behavior, which is found in both ordered and disordered phases, and both near and away from the magnetic transition, remains a major unsolved problem. We derive and discuss three novel mechanisms underlying such behavior that are based on electron scattering mediated by the exchange of (1) ferromagnons or (2) skyrmionic fluctuations, both in conjunction with weak disorder, or (3) helimagnons in clean systems. Since the magnetic transition in weakly disordered sytems is generically discontinuous, static droplets of the ordered phase can exist within the disordered phase, making the mechanisms viable there as well. We compare our theoretical results with existing experimental ones and suggest additional experiments.

I. INTRODUCTION, AND RESULTS

A. Non-Fermi-liquid behavior in magnets

A characteristic property of Fermi liquids is a low-temperature (T) electrical resisitivity ρ of the form $\delta\rho(T \to 0) \propto T^2$, with $\delta\rho = \rho - \rho_0$ the T-dependent part of the resistivity and ρ_0 the residual resistivity;[1] this behavior is realized in simple metals.[2,3] A resistivity that does not satisfy this law is one of the hallmarks of metals referred to as non-Fermi liquids (NFLs). An obvious cause for NFL behavior is the vicinity of a quantum critical point, where the critical dynamics can lead to an unusual time and temperature dependence of various correlation functions.[4,5] More puzzling are examples where the NFL behavior is observed in large regions of the phase diagram, even far from any phase transition. One such class of NFL materials is comprised of metallic ferromagnets (FMs) and helimagnets (HMs). The NFL behavior can occur in either the magnetically ordered or disordered phases, or in both, and it is characterized by a T^s behavior

$$\delta\rho(T \to 0) = A_s T^s \tag{1.1}$$

with an exponent s that is commonly observed to be $3/2 \lesssim s < 2$. Examples include the ferromagnets $ZrZn_2$,[6] Ni_3Al tuned by either doping with Pd[7] or pressure,[8] and $Ca_xSr_{1-x}RuO_3$,[9] all of which display a power-law T-dependence of $\delta\rho$ with an exponent s that is clearly smaller than 2 on either side of the quantum FM transition. Another example is the HM MnSi, which is tunable by pressure and displays a $T^{3/2}$ behavior over a temperature range of nearly three decacdes in a large region in the disordered phase, with a remarkably large prefactor $A_{3/2}$, but T^2 behavior in the ordered phase.[10] These systems all fulfill two requirements that help rule out possible reasons for the NFL behavior: (1) They are relatively clean, as evidenced by a small value of ρ_0, or a large mean-free path. This rules out effects due to diffusive electron dynamics that can lead to NFL behavior.[11,12] (2) The NFL behavior is generic, i.e., it is observed in large regions of the phase diagram, which rules out the possible influence of quantum critical behavior. In Figs. 1, 2 we show the schematic phase diagrams of $ZrZn_2$ and MnSi, respectively, for illustrative purposes. Notice that the exponent s for $ZrZn_2$ takes on its smallest value of 1.5 in a pocket around $T = 10$K and $p = 2$GPa, but is close to 1.7 in a large part of the phase diagram. This somewhat ill-defined value of s suggests that several competing scattering mechanisms lead to an effective power law. In MnSi, by contrast, a very clean $T^{3/2}$ behavior is observed over more than two temperature decades, which suggests one dominating scattering mechanism. There are other examples, such as $Nb_{1-y}Fe_{2+y}$,[17] $NiGa_3$,[14,18] and $(Ni_{1-x}Pd_x)_3Al$,[7] that allow for more possibilities since they lack one or both of these requirements; we will come back to some of these in the discussion.

In the context of requirement (2), and for later reference, we mention that it is now well understood theoretically,[19,20] and confirmed experimentally,[21] that the quantum phase transition in clean metallic FMs is generically discontinuous or first order, so by definition there is no standard magnetic quantum critical behavior. This is indeed the case for all of the FM examples listed above, and also for MnSi. Requirement (2) is still useful, however, as critical fluctuations may be found in a pre-asymptotic region in the vicinity of a transition that is weakly first order. We also mention that phase separation is routinely observed away from the coexistence curve in systems that display a first-order transition,[22–24] which means that each phase displays, to some extent, characteristics of the other phase. We will come back to this phenomenon, as it is crucial for some of our arguments.

The generic NFL behavior summarized above has proved very challenging to explain, and is still far from understood. One mechanism leading to a $T^{3/2}$ behavior

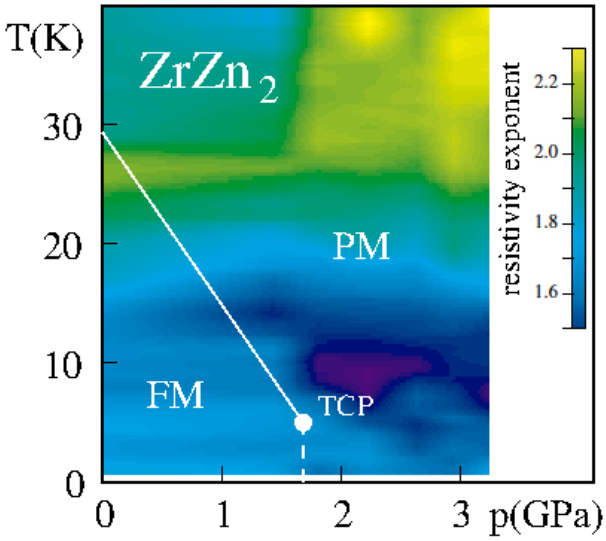

Figure 1: Experimental temperature-pressure phase diagram of $ZrZn_2$ showing the ferromagnetic (FM) and paramagnetic (PM) phases. The tricritical point (TCP) separates the line of second-order transitions (solid) from the line of first-order transitions (dashed). The false colors indicate the exponent s that characterizes the power-law T dependence of the electrical resistivity $\delta\rho$. After Ref. 6.

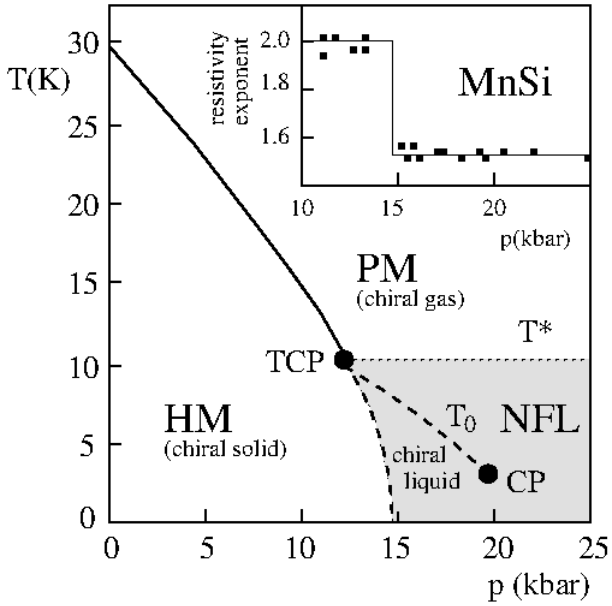

Figure 2: Temperature-pressure phase diagram of MnSi combining experimental data from Refs. 13–15 with theoretical interpretations from Ref. 16. HM and PM are the helimagnetic and paramagnetic phases, respectively. The tricritical point (TCP) separates the line of second-order transitions (solid) from a line of first-order transitions (dashed). The shaded area is the NFL region; its upper limit (dotted line, T^*) is not sharp. The observed resistivity exponent value changes abruptly at the critical pressure as shown in the inset. The region below T_0 is where Ref. 15 found partial helical order. This was interpreted in Ref. 16 as a chiral liquid, separated from the chiral gas above T_0 by a first-order transition that ends in a critical point (CP). See the text for further information.

that is applicable to HMs was reported in Ref. 25, where it was shown that scattering of electrons by columnar fluctuations (which in HMs can be realized by skyrmionic spin textures, see Ref. 26) in conjunction with weak quenched disorder leads to a $T^{3/2}$ behavior of the electrical resistivity.

The fact that similar NFL behavior has been found in various FMs implies that the above mechanism, which vanishes in the FM limit $q \to 0$, is not sufficiently general to explain all of the observations. In addition, the exponent observed in MnSi is $s = 1.5$ over several decades of temperatures,[10] whereas the exponents observed in FMs, while clearly less than 2, tend to be slightly larger than 1.5, and the smallest values of s are not necessarily observed at the lowest temperatures, see Fig. 1. Also, in MnSi the NFL behavior is observed in the disordered phase only, whereas in the various ferromagnets it is found in either phase. All of this indicates that different mechanisms may be at work in different materials. The observed NFL transport properties of low-temperature FMs and HMs thus remains a major unsolved problem.

In this paper we derive and discuss three additional mechanism that lead to a $T^{3/2}$ NFL behavior of the electrical resistivity. The first one relies on FM order and involves magnon-mediated scattering of electrons in different subbands of the exchange-split conduction band (interband scattering) in the presence of weak disorder. The second mechanism is applicable to HMs with skyrmionic spin textures, where interband scattering in conjuction with weak disorder leads, in a large pre-asymptotic temperature region, to a $T^{3/2}$ behavior. The third one involves HMs without skyrmions and does not require any quenched disorder. It involves scattering of electrons in different subbands with the interaction mediated by helimagnons. We compare and contrast these mechanisms with the one previously reported in Ref. 25, and also with various competing scattering mechanisms that lead to different power laws.

This paper is organized as follows: In the remainder of this section we summarize our main results. In Sec. II we discuss some general physical principles that allow for very simple derivations of our results, which are given in Sec. III. We discuss our results and the experimental situation in Sec. IV.

B. Summary of main results

For the convenience of the reader we first summarize our main results; see also Table I. We have identified three mechanisms that lead to a $T^{3/2}$ behavior of the electrical resistivity in sizable temperature regimes, namely:

1. Mechanism 1: Magnon-mediated scattering in weakly disordered ferromagnets

The first mechanism relies on FM order. It involves magnon-mediated scattering of electrons in different subbands of the exchange-split conduction band (interband scattering) in the presence of weak disorder (ballistic regime, see Refs. 27 and 28,29). In the current context, weak disorder is defined by the inequalities $\lambda\tau \gg 1$ and $T \gg T_{\rm ball} \equiv T_1/(\epsilon_{\rm F}\tau)^2$, with λ the exchange splitting of the conduction band, T_1 the magnon energy at the edge of the Brillouin zone (i.e., the magnetic Debye temperature), $\epsilon_{\rm F}$ the Fermi energy, and τ the elastic mean-free time that determines the residual resistivity. The result for $\delta\rho$ for this case can be written

$$\delta\rho_{\rm FM}/\rho_0 = \gamma_1 T^{3/2}/T_1\sqrt{T_0}\ , \qquad (1.2)$$

with γ_1 a numerical constant. It is valid for $T_{\rm ball} \ll T \lesssim T_0$, with $T_0 = T_1\lambda^2/\epsilon_{\rm F}^2$. Equation (1.2) also holds for the thermal resistivity, only the numerical prefactor is different.

2. Mechanism 2: Skyrmionic columnar fluctuations in helimagnets with weak disorder

The second mechanism is applicable to HMs with skyrmionic spin textures comprised of three helices with pitch wave number q, as proposed in Ref. 26. Fluctuations of the resulting columnar order lead, in conjuction with weak disorder and for interband scattering, to a result that is identical to the one in weakly disordered FMs,

$$\delta\rho_{\rm sky}/\rho_0 = \gamma_2 T^{3/2}/T_1\sqrt{T_0}\ , \qquad (1.3)$$

with γ_2 another constant. The prefactor of the $T^{3/2}$ law is much larger than the one found previously for intraband scattering mediated by columnar fluctuations.[25] This result is valid for $T_{\rm ball} \ll T \lesssim T_0$, except that for temperatures lower than $T_1(q/k_{\rm F})^4$ it crosses over to a $T^{5/4}$ behavior (provided the crossover temperature is larger than $T_{\rm ball}$). It also holds for both the electrical and the thermal resistivity.

3. Mechanism 3: Helimagnon-mediated scattering in clean helimagnets

The third mechanism is applicable to HMs, and does not rely on quenched disorder. It involves interband scattering of electrons mediated by helimagnons. While the dominant contribution at asymptotically low T is given by the scattering of electrons in the same subband (intraband scattering, see Refs. 29,30), this mechanism provides the leading contribution in a pre-asymptotic temperature window. The result is

$$\delta\rho_{\rm HM}/\rho_0 = \gamma_3\,(q/k_{\rm F})\,\lambda\tau\,(T/T_1)^{3/2}\ . \qquad (1.4)$$

Here q is the pitch wave number of the helically ordered phase, and γ_3 is a third constant. Equation (1.4) is valid for $q/k_{\rm F} \ll 1$ and $T_0 \lesssim T \lesssim T_1(q/k_{\rm F})^2$ (provided this temperature window exists). This result holds for the electrical resistivity, the contribution to the thermal resistivity is proportional to T.

II. GENERAL CONSIDERATIONS

All of the mechanisms discussed in this paper hinge on three basic observations. The first one is that any nonanalytic T-dependence of $\delta\rho$ requires the existence of soft or massless modes that are infinitely long lived in the limit of long wavelengths and couple to the conduction electrons.

The second observation is that in any metallic magnet the Fermi surface is split by the exchange splitting λ. In general one thus expects two types of scattering processes. One is scattering between electrons in different subbands (interband scattering). In clean systems, these processes will be exponentially frozen out at low temperatures, so any power law generated by an exchange of soft modes must cross over to an exponentially small rate at asymptotically low temperatures. A second type of processes is scattering between electrons in the same subband (interband scattering). These can produce power laws even at arbitrarily low temperatures, and hence will asymptotically always dominate the interband processes. However, as we will see, this argument may be irrelevant for practical purposes, since small prefactors can make the asymptotic low-temperature region unobservably small, and small amounts of quenched disorder can qualitatively change the behavior. Also, in ferromagnets intraband scattering is absent since ferromagnetic magnons do not couple electrons in the same subband.

The third observation is that in the vicinity of a first-order transition, as is realized at low T in all of the magnets under discussion (see above), phase separation, i.e., the existence of a finite fraction of the ordered phase within the disordered one, and vice versa, is commonly observed; see Refs. 22–24 for examples involving some of the magnets under discussion here. This has recently been explained by the realization that static, finite-size droplets of the minority phase are stable within the majority phase on either side of the coexistence curve, provided there is a moderate amount of quenched disorder that couples predominantly to the order-parameter degrees of freedom, in this case the magnetization.[31] This allows features that are characteristic of one phase to exist, to a limited extent, on both sides of the coexistence curve. This will play an important role in our discussions.

We now discuss the relevant soft modes and energy scales, and provide basic expressions for scattering rates that can be used to derive all of our results.

A. Goldstone modes, and susceptibilities

An obvious soft mode in a FM is the ferromagnon with dispersion relation[3]

$$\omega_{\rm FM}(\boldsymbol{k}\to 0) = D\boldsymbol{k}^2 \tag{2.1}$$

with D the spin-stiffness coefficient.

The corresponding Goldstone mode in the helical phase of a HM is the helimagnon with dispersion relation[32]

$$\omega_{\rm HM}(\boldsymbol{k}\to 0) = \sqrt{c_2 k_z^2 + c_4 \boldsymbol{k}_\perp^4}\ , \tag{2.2a}$$

with k_z and $\boldsymbol{k}_\perp$ the components of $\boldsymbol{k}$ parallel and perpendicular, respectively, to the pitch wave vector $\boldsymbol{q}$. In the limit of a long pitch wavelength, $q/k_F \ll 1$, one has $c_2 \propto c_4\, q^2$ with $c_4 \propto D^2$. Ignoring numerical prefactors, we have

$$\omega_{\rm HM}(\boldsymbol{k}) = D\sqrt{q^2 k_z^2 + \boldsymbol{k}_\perp^4} \quad (k \lesssim q)\ . \tag{2.2b}$$

This is valid for $k \lesssim q$; in the opposite limit the resonance frequency crosses over to the ferromagnetic one.

Finally, in a phase with columnar order the Goldstone modes are columnar fluctuations with a dispersion relation of the form[33,34]

$$\omega_{\rm col}(\boldsymbol{k}) = \sqrt{c_4 k_z^4 + c_2 \boldsymbol{k}_\perp^2}\ . \tag{2.3a}$$

An example of columnar order in a magnet is the skyrmion spin texture observed in the A-phase of the HM MnSi.[26] If the skyrmions are comprised by a superposition of three helices, as proposed in Ref. 26, one has again $c_2 \propto c_4 q^2 \propto D^2 q^2$, and ignoring numerical prefactors we write

$$\omega_{\rm sky}(\boldsymbol{k}) = D\sqrt{k_z^4 + \boldsymbol{k}_\perp^2 q^2} \quad (Dq^4/k_{\rm F}^2 \lesssim \omega_{\rm sky} \lesssim Dq^2)\ . \tag{2.3b}$$

The region of validity of this expression is bounded above by $k \approx q$ or $\omega \lesssim Dq^2$; for larger k the frequency again crosses over to the ferromagnetic one. It is bounded below by $\omega \gtrsim Dq^4/k_{\rm F}^2$; for asymptotically small frequencies the dynamics of the soft modes change and one obtains[35]

$$\omega_{\rm sky}(\boldsymbol{k}) = D(k_{\rm F}^2/q^2)\left(k_z^4/q^2 + \boldsymbol{k}_\perp^2\right) \quad (\omega_{\rm sky} \lesssim Dq^4/k_{\rm F}^2)\ . \tag{2.3c}$$

We will refer to all of these Goldstone modes arising from magnetic order summarily as "magnons". For deriving their contributions to the electronic relaxation rates, we consider the effective interaction between electrons mediated by the exchange of magnons, see Fig. 3. The effective potential is proportional to the susceptibility χ of the order-parameter phase fluctuations that also determine the Goldstone propagator. In the case of the FM these phase fluctuations are simply the transverse components of the magnetization. In the HM case they are a generalized phase that involves a transverse gradient that leads to the characteristic anisotropic dispersion

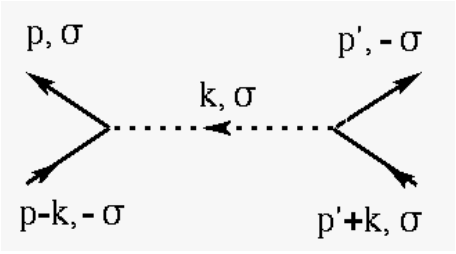

Figure 3: Effective interband scattering of electrons mediated by magnon exchange. The effective potential is represented by the dotted line, and $\sigma = \pm 1 \equiv \uparrow, \downarrow$ is the spin projection.

relation for the helimagnons.[32] The leading contribution to χ in FMs and in the helical and columnar phases of HMs, respectively, apart from a numerical prefactor, is given by the following expressions (see Refs. 30,36, and also Sec. IV A).

FM:

$$\chi(\boldsymbol{k}, i\Omega) \propto \frac{m_0 D\boldsymbol{k}^2}{\omega_{\rm FM}(\boldsymbol{k})^2 - (i\Omega)^2}\ , \tag{2.4a}$$

HM helical:

$$\chi(\boldsymbol{k}, i\Omega) \propto \frac{m_0 D\boldsymbol{q}^2}{\omega_{\rm HM}(\boldsymbol{k})^2 - (i\Omega)^2}\ , \tag{2.4b}$$

HM skyrmionic:

$$\chi(\boldsymbol{k}, i\Omega) \propto \begin{cases} \frac{m_0 D\boldsymbol{q}^2}{\omega_{\rm sky}(\boldsymbol{k})^2 - (i\Omega)^2} & \text{for } \omega_{\rm sky} \gtrsim Dq^4/k_{\rm F}^2 \\ \frac{m_0 (k_{\rm F}/q)^2 \omega_{\rm sky}(\boldsymbol{k})}{\omega_{\rm sky}(\boldsymbol{k})^2 - (i\Omega)^2} & \text{for } \omega_{\rm sky} \lesssim Dq^4/k_{\rm F}^2\ . \end{cases} \tag{2.4c}$$

Here m_0 is the magnetization scale, i.e., the expectation value of the local spin density, and we neglect the damping of the magnons. Note that in a FM the numerator is proportional to a gradient squared, while in the HM helical case this is replaced by a q^2. As a result, the HM helical susceptibility is softer than the FM one, even though the HM helical resonance frequency is stiffer than the FM one.

B. Energy scales

For later reference we discuss various energy scales that are relevant for the problem at hand. The highest of these is the microscopic or atomic energy scale E_a. In good metals this is usually the Fermi energy,[37] which we denote by $\epsilon_{\rm F}$. The magnetism is characterized by several closely related energy scales. One is given by the maximum excitation energy,

$$T_1 = D/a^2 \approx Dk_{\rm F}^2\ , \tag{2.5}$$

with a the microscopic length scale, which in good metals is close to the inverse of the Fermi wave number $k_{\rm F}$. T_1 is the magnetic analog of a Debye temperature. A

second one is the exchange splitting λ, which is due to the effective magnetic field seen by the conduction electrons. It is related to the magnetization scale m_0 via the exchange interaction Γ_t that couples the electronic spin to the magnetization:[38]

$$\lambda = \Gamma_t m_0 \ . \tag{2.6}$$

A third relevant scale arises in interband scattering processes. The smallest wave number that can be transferred by means of magnon exchange is on the order of $k_0 = \lambda/v_\mathrm{F}$, with v_F the Fermi wave number, and the smallest energy that can be transferred is therefore

$$T_0 = Dk_0^2 \approx T_1 \left(\lambda/\epsilon_F\right)^2 \ . \tag{2.7}$$

Another energy scale is relevant in HMs. The expression (2.2b) is valid only for $k < q$; for larger wave numbers they cross over to a ferromagnetic dispersion relation. The temperature region where these excitations determine the scaling of the scattering rates is thus bounded above by

$$T_q = Dq^2 = T_1 (q/k_\mathrm{F})^2 \ . \tag{2.8}$$

Finally, consider quenched disorder as characterized by an elastic scattering time τ. We will be interested in the ballistic regime,[27] which is separated from the diffusive regime by the requirement $v_\mathrm{F} k > 1/\tau$, with k the momentum transfer in the scattering process (or, alternatively, by $k\ell > 1$, with ℓ the elastic mean-free path). The magnon frequency scales as the temperature, and from Eqs. (2.1, 2.2b, 2.3b) we see that in all of these cases the wave number squared scales as the magnon frequency divided by D, i.e., the wave number scales as $k \sim \sqrt{T/D}$. The ballistic transport regime is therefore restricted to temperatures $T > T_\mathrm{ball}$, where

$$T_\mathrm{ball} = T_1/(\epsilon_\mathrm{F}\tau)^2 \ . \tag{2.9}$$

We will be interested in situations where T_0 and T_ball are well separated, $T_\mathrm{ball} \ll T_0$, which requires the weak-disorder condition $\lambda\tau \gg 1$.

C. General expressions for the scattering rates

We now provide expressions for the scattering rates in terms of integrals, first for the single-particle rate $1/\tau_\mathrm{sp}$ in clean systems, for both interband and intraband scattering. $1/\tau_\mathrm{sp}$ determines the thermal resistivity.[2] The electrical resistivity is determined by the transport rate $1/\tau_\mathrm{tr}$. It is well known that in clean systems the latter differs from the former by a factor in the integrand that suppresses backscattering and is proportional to the momentum transfer squared, or $(\boldsymbol{k}-\boldsymbol{p})^2/k_\mathrm{F}^2$ in Eqs. (2.10, 2.11) below.[2] We will later use this observation to deduce the transport rate from the single-particle one. Together with simple arguments about the effects of disorder this will suffice to obtain both rates, and hence both the thermal and the electrical resistivity, for all cases of interest by just considering the single-particle rate in clean systems.

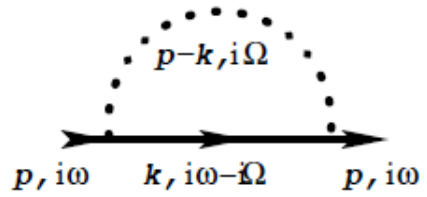

Figure 4: Exchange contribution to the single-particle self energy that results from the interaction vertex shown in Fig. 3.

1. *Single-particle rate, clean systems*

a) Interband scattering We start with an expression for the single-particle relaxation rate $1/\tau_\mathrm{sp}$ due to magnon exchange between electrons in different subbands of the exchange-split conduction band (interband scattering) in clean systems. For a quasiparticle with wave vector $\boldsymbol{k}$ it is given by the imaginary part of the Fock or exchange contribution to the quasiparticle self energy shown in Fig. 4. Averaging over the Fermi surface, and remembering that the effective potential is proportional to the phase-fluctuation susceptibility, we find, apart from purely numerical prefactors,

$$\frac{1}{\tau_\mathrm{sp}} \ \propto \ N_\mathrm{F}\Gamma_t^2 \int du \ \frac{1}{\sinh(u/T)} \frac{1}{N_\mathrm{F}^2 V^2} \sum_{\boldsymbol{k},\boldsymbol{p}} \delta(\xi_{\boldsymbol{k}} - \lambda) \times \delta(\xi_{\boldsymbol{p}} + \lambda)\, \chi''(\boldsymbol{k}-\boldsymbol{p}, u) \tag{2.10}$$

Here $\xi_{\boldsymbol{k}} = 0$ defines the Fermi surface in the absence of an exchange splitting, V is the system volume, and χ'' is the spectrum of the susceptibility given in Eqs. (2.4). The two δ-functions pin the electrons to the respective Fermi surfaces. With χ representing the FM susceptibility, Eq. (2.4a), this expression was considered in Ref. 36; it also holds for the two helical cases.

b) Intraband scattering We now consider magnon exchange between electrons in the same subband (intraband scattering). This is relevant only for the helical cases; in ferromagnets the magnons do not couple electrons in the same subband. The expression for the single-particle relaxation rate was derived in Refs. 32 and 28. The result is very similar to Eq. (2.10); it takes the form

$$\frac{1}{\tau_\mathrm{sp}} \ \propto \ N_\mathrm{F}\Gamma_t^2 \left(\frac{q}{k_\mathrm{F}}\right)^2 \left(\frac{\epsilon_\mathrm{F}}{T_1}\right)^2 \int du \ \frac{1}{\sinh(u/T)} \frac{1}{N_\mathrm{F}^2 V^2} \sum_{\boldsymbol{k},\boldsymbol{p}} \times \delta(\xi_{\boldsymbol{k}})\, \delta(\xi_{\boldsymbol{p}}) \, \frac{(\boldsymbol{k}-\boldsymbol{p})^2}{k_\mathrm{F}^2} \, \chi''(\boldsymbol{k}-\boldsymbol{p}, u) \tag{2.11}$$

The δ-functions now reflect the fact that both electrons belong to the same Fermi surface. The extra factor of $(\boldsymbol{k}-\boldsymbol{p})^2$ compared to Eq. (2.10) is due to the fact that electrons in the same band can couple only to gradients of the fluctuating phase, whereas electrons in different bands couple to the phase directly.[39]

2. Transport rate, clean systems

A determination of the electrical resistivity requires solving the Boltzmann equation, or, equivalently, evaluating the Kubo formula. Even in the simplest conserving approximation this requires solving an integral equation for a vertex function. This integral equation is usually replaced by an algebraic equation.[40] In Ref. 41 it was shown that this approximation is exact with respect to the leading low-temperature dependence of the resistivity, and the resulting algebraic equations for FMs were derived and solved in Ref. 36. The final result is as follows: The electrical resistivity is effectively given by the transport rate $1/\tau_{\rm tr}$, which is obtained from the same integral as the single-particle rate, Eqs. (2.10, 2.11), but with an additional factor of $(\boldsymbol{k}-\boldsymbol{p})^2/k_{\rm F}^2$ in the integrand. In the context of the Boltzmann equation this is known as the backscattering factor; it suppresses large-angle scattering and thus weakens the temperature dependence of the transport rate compared to the single-particle rate.[2] With the exception of the skyrmionic case at asymptotically low frequencies, the wave number squared scales as the Goldstone-mode frequency for all of the cases we are considering, see Sec. II A, which in turn scales as the temperature. We can thus immediately anticipate that generically the leading T-dependence of the transport rate will have an additional factor of T compared to the single-particle rate. The only caveat is that this argument assumes that the final integrals are infrared convergent once the temperature has been scaled out; this is not always the case, see Sec. III C below.

3. Effects of disorder

The effects of weak quenched disorder are qualitatively different depending on whether we consider interband or intraband scattering. A complete discussion requires evaluating the Kubo formula with impurity scattering taken into account. The leading contribution to the electron self energy in the weak or ballistic disorder regime, $\lambda\tau \gg 1$, is shown in Fig. 5, and the leading contributions to the electrical conductivity are shown in Fig. 6; see Refs. 28,29 for a complete discussion for the case of helimagnon-mediated scattering. However, for the cases of interest here a much simpler argument suffices; we discuss its relation to the detailed calculation in the Appendix.

a) Interband scattering Consider the expression for the clean single-particle rate given in Eq. (2.10). Shifting the momentum $\boldsymbol{k}$ by $\boldsymbol{p}$ and performing the $\boldsymbol{p}$-integration yields

$$\frac{1}{N_{\rm F}V}\sum_{\boldsymbol{p}}\delta(\xi_{\boldsymbol{k}+\boldsymbol{p}}-\lambda)\,\delta(\xi_{\boldsymbol{p}}+\lambda) \;\propto\; \int_{-1}^{1} d\eta\,\delta(kv_{\rm F}\eta-2\lambda) = \frac{1}{v_{\rm F}k}\,\Theta(k-2\lambda/v_{\rm F})\;. \quad (2.12)$$

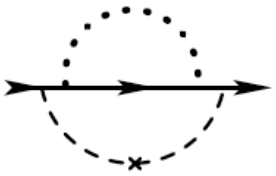

Figure 5: Leading contributions to the electron self energy in the weak-disorder or ballistic regime. The dotted line represents the effective interaction mediated by the magnons; the dashed line with a cross represents the quenched impurities.

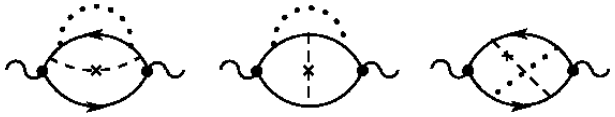

Figure 6: Leading contributions to the conductivity in the weak-disorder or ballistic regime. Dotted lines represent the effective interaction mediated by the magnons; dashed lines with crosses represent the quenched impurities. The dots represent the external current vertices.

Note the theta function, which leads to an exponentially small scattering rate at asymptotically low temperatures.[36] Weak disorder smears out the δ-function and we have, in the limit $v_{\rm F}k \ll \lambda$ and $\lambda\tau \gg 1$,

$$\frac{1}{v_{\rm F}k}\,\Theta(k-2\lambda/v_{\rm F}) \;=\; \int_{-1}^{1} d\eta\,\delta(v_{\rm F}k\eta-2\lambda) \;\to\; \int_{-1}^{1} d\eta\;\frac{1/\tau}{(v_{\rm F}k\eta-2\lambda)^2+1/\tau^2} \approx \frac{1}{\lambda^2\tau}\;. \quad (2.13)$$

The disorder thus results in, (1) an extra factor of $v_{\rm F}k/\lambda^2\tau$ in the integrand, and (2) the elimination of the step function, and hence of the lower cutoff for the k-integral. Since k scales as $k \sim T^{1/2}$, this means that disorder leads to a power-law temperature dependence of $1/\tau_{\rm sp}$ that is *weaker* than in the clean case by a factor of $T^{1/2}$, but extends to temperatures below the energy scale T_0.

For the transport rate, disorder eliminates the backscattering factor since it leads to more isotropic scattering. The effective extra factor in the integrand is thus $(\epsilon_{\rm F}/\lambda^2\tau)k_{\rm F}/k$, and disorder *strengthens* the temperature dependence of the rate by a factor of $1/T^{1/2}$. As a result, the single-particle rate and the transport rate display the same temperature dependence. Again, these conclusions may be modified by the convergence properties of the final dimensionless integrals.

b) Intraband scattering In the case of intraband scattering the arguments of the δ-functions in Eq. (2.12) are not shifted with respect to one another, and the smearing

argument yields

$$\frac{1}{v_{\rm F}k} \;=\; \int_{-1}^{1} d\eta\, \delta(v_{\rm F}k\eta)$$
$$\to \int_{-1}^{1} d\eta\, \frac{1/\tau}{(v_{\rm F}k\eta)^2+1/\tau^2} \approx \frac{1}{v_{\rm F}k}\left[1-\frac{1}{v_{\rm F}k\tau}\right] . \qquad (2.14)$$

Disorder thus provides a correction to the scattering rate that comes with an extra factor of $1/v_{\rm F}k\tau$ in the integrand and *strengthens* the temperature dependence of $1/\tau_{\rm sp}$ by a factor of $1/T^{1/2}$. The sign of this contribution is negative, and it always is a small correction to the clean contribution (since $T > T_{\rm ball}$). For the transport rate the backscattering factor is suppressed in addition, and disorder strengthens the T-dependence of the rate by a factor of $1/T^{3/2}$. The disorder corrections to both rates thus again have the same temperature dependence.

The above simple argument always yields the correct temperature scaling of both rates for all of the cases considered here. However, the sign of the disorder correction is rendered correctly only for the skyrmionic case, whereas intraband scattering by helimagnons results in a positive disorder correction to the rates.[28,29] The reason is that in this case the simple factor of $(\boldsymbol{k}-\boldsymbol{p})^2$ in Eq. (2.11) does not adequately describe the coupling of the Goldstone modes to the electrons. The actual coupling contains an angular dependence that flips the sign, as explained in the Appendix.

All of these observations are consistent with the results of the explicit calculations in Refs. 28,29.

III. DERIVATIONS

We are now in a position to provide very simple derivations of the contributions to the scattering rates, and hence the electrical and thermal resistivities, due to the exchange of ferromagnons, skyrmionic columnar fluctuations, or helimagnons, with or without weak quenched disorder, and involving either interband or intraband scattering.

A. Mechanism 1: Magnon-mediated scattering in weakly disordered ferromagnets

For ferromagnets only the interband scattering mechanism is relevant; the magnons do not couple electrons in the same subband. For clean systems the single-particle rate is given by Eq. (2.10). With Eqs. (2.4a) and (2.1) for the susceptibility and the magnon frequency, respectively, we have

$$\frac{1}{\tau_{\rm sp}} \;\propto\; \frac{\lambda}{N_{\rm F}V}\sum_{\boldsymbol{k}} \frac{1}{\sinh(Dk^2/T)} \int_{-1}^{1} d\eta\; \delta(kv_{\rm F}\eta-2\lambda)$$
$$= \;\frac{\lambda}{N_{\rm F}V}\sum_{\boldsymbol{k}} \frac{1}{\sinh(Dk^2/T)}\,\frac{1}{v_{\rm F}k}\,\Theta(k-2\lambda/v_{\rm F})$$
$$\propto\; \frac{T\lambda}{T_1}\int_{T_0/T}^{T_1/T} dx\,\frac{1}{\sinh x}\;, \qquad (3.1)$$

where we have dropped a factor of $N_{\rm F}\Gamma_t = O(1)$, as we have all other numerical prefactors. We thus reproduce the result of Ref. 36:

$$\frac{1}{\tau_{\rm sp}} \propto (T\lambda/T_1)\times\begin{cases} e^{-T_0/T} & \text{for}\quad T\lesssim T_0 \\ \ln(T/T_0) & \text{for}\quad T_0\lesssim T\lesssim T_1\;. \end{cases} \qquad (3.2)$$

The corresponding result for $1/\tau_{\rm tr}$ is $T^2\lambda/T_1^2$ for $T_0 \lesssim T \lesssim T_1$, and an exponentially small expression for $T \lesssim T_0$.[36] Now consider weak disorder, characterized by $\lambda\tau \gg 1$. As explained in Sec. II C 3, the integrand in Eq. (3.1) acquires, in the region $v_{\rm F}k \ll \lambda$, an additional factor of $v_{\rm F}k/\lambda^2\tau$, and the step function disappears. Ballistic disorder thus leads to an additional contribution to the single-particle rate

$$\delta(1/\tau_{\rm sp}) \;\propto\; \frac{1}{\lambda\tau N_{\rm F}}\,\frac{1}{V}\sum_{\boldsymbol{k}}\frac{1}{\sinh(Dk^2/T)}\,\Theta(\lambda-kv_{\rm F})$$
$$\propto\; \frac{1}{\tau}\,\frac{\epsilon_{\rm F}}{\lambda}\left(\frac{T}{T_1}\right)^{3/2}\int_0^{T_0/T} dx\,\frac{\sqrt{x}}{\sinh x}\;. \qquad (3.3a)$$

For $T \gg T_0$ this gives a small correction to the clean rate, Eq. (3.2), but for $T \lesssim T_0$ it provides the leading contribution, which is proportional to $T^{3/2}$. The result for the transport rate is the same, as explained in Sec. II C 3, and we obtain

$$\delta(1/\tau_{\rm tr}) \propto \delta(1/\tau_{\rm sp}) \propto \frac{1}{\tau}\,\frac{\epsilon_{\rm F}}{\lambda}\left(\frac{T}{T_1}\right)^{3/2} \qquad (T\lesssim T_0)\;. \qquad (3.3b)$$

This is equivalent to Eq. (1.2), which holds for both the electrical resistivity, which is given by $1/\tau_{\rm tr}$, and the thermal resistivity, which is given by $1/\tau_{\rm sp}$.

These results are summarized in Table I.

B. Mechanism 2: Skyrmionic columnar fluctuations in helimagnets with weak disorder

Columnar fluctuations of any kind have a resonance frequency of the form given in Eq. (2.3a). If the columns are formed by skyrmionic spin textures that result from a superposition of three helices with pitch wave number q, as was proposed in Ref. 26, then the resonance frequency is given by Eq. (2.3b) in the sizable frequency window $T_q\, q^2/k_{\rm F}^2 \lesssim \omega \lesssim T_q$, and by Eq. (2.3c) for asymptotically small frequencies or wave numbers. The relevant

susceptibility in these two regimes is given by Eq. (2.4c). Repeating the calculation from Sec. III A we then obtain for the single-particle rate due to interband scattering in clean systems

$$\frac{1}{\tau_{\rm sp}} \propto \frac{T\lambda}{T_1}\int_{\sqrt{T_0/T}}^{\sqrt{T_1/T}} \frac{dz}{z}\int_0^\infty dx\,\frac{1}{\sqrt{z^4+x}}\,\frac{1}{\sinh\sqrt{z^4+x}} \propto \begin{cases}(T^2\lambda/T_0T_1)e^{-T_0/T} & \text{for} \quad T\lesssim T_0\\ (T\lambda/T_1)\ln^2(T/T_0) & \text{for} \quad T_0\lesssim T\lesssim T_q\end{cases}. \tag{3.4}$$

The second temperature window may or may not exist, depending on the relative values of T_0 and T_q. For $T\gtrsim T_q$ the result crosses over to the FM one. The corresponding result for $1/\tau_{\rm tr}$ is exponentially small and $T^2\lambda/T_1^2$, respectively, in the two temperature regions. In the presence of ballistic disorder both rates go as $T^{3/2}$ by the same arguments as in the FM case, and we obtain

$$\delta\left(1/\tau_{\rm tr}\right)\propto\delta\left(1/\tau_{\rm sp}\right) \propto \frac{1}{\tau}\frac{\epsilon_{\rm F}}{\lambda}\left(\frac{T}{T_1}\right)^{3/2} \left(\mathrm{Max}(T_{\rm ball}, T_q\,q^2/k_{\rm F}^2)\lesssim T\lesssim T_q\right). \tag{3.5}$$

This result is equivalent to Eq. (1.3). For $T\gtrsim T_q$ it crosses over to the FM result, so ignoring the numerical prefactor it effectively is valid for temperatures $T\lesssim \mathrm{Max}(T_q,T_0)$.

For asymptotically small frequencies or wave numbers the resonance frequency and the phase susceptibility are given by Eq. (2.3c) and the second expression in (2.4c), respectively. Repeating the calculation for this case we find

$$\delta\left(1/\tau_{\rm tr}\right)\propto\delta\left(1/\tau_{\rm sp}\right) \propto \frac{1}{\tau}\frac{\epsilon_{\rm F}}{\lambda}\frac{q}{k_{\rm F}}\left(\frac{T}{T_1}\right)^{5/4} \left(\tilde{T}_{\rm ball}\lesssim T\lesssim T_q\,q^2/k_{\rm F}^2\right). \tag{3.6}$$

Here $\tilde{T}_{\rm ball}=T_{\rm ball}\,(k_{\rm F}/q)^4/(\epsilon_{\rm F}\tau)^2$. We note that in HMs such as MnSi, $q/k_{\rm F}$ tends to be on the order of 10^{-2}. The temperature $T_q\,q^2/k_{\rm F}^2$ where this asymptotic behavior sets in therefore tends to be extremely low, and not necessarily larger than either $T_{\rm ball}$ or $\tilde{T}_{\rm ball}$, so the temperature window where Eq. (3.6) is valid may not exist.

For intraband scattering in clean systems, analogous considerations using Eq. (2.11) readily show that the single-particle and transport rates scale as T^2 and T^3, respectively, in the pre-asymptotic region $T_q\,q^2/k_{\rm F}^2\lesssim T\lesssim T_q$, which crosses over to $T^{3/2}$ and T^2, respectively in the asymptotic region $T_{\rm ball}\lesssim T\lesssim T_q\,q^2/k_{\rm F}^2$. The disorder correction to either rate scales as $T^{3/2}$ in the pre-asymptotic region, but it always is a small correction to the clean contribution, as explained in Sec. II C 3. Asymptotically this crosses over to a $T^{5/4}$ correction.

All of these results are summarize in Table I.

C. Mechanism 3: Helimagnon-mediated scattering in clean helimagnets

In clean HMs, the leading helimagnon contribution to the relaxation rates at asymptotically low temperatures comes from interband scattering. Using Eqs. (2.2b) and (2.4b) in Eq. (2.11) we reproduce the result of Ref. 30 for the single-particle rate:

$$\frac{1}{\tau_{\rm sp}}\propto\lambda\left(\frac{q}{k_{\rm F}}\right)^6\left(\frac{\epsilon_{\rm F}}{T_1}\right)^2\left(\frac{T}{T_q}\right)^{3/2}. \tag{3.7}$$

The transport rate is given by the same expression with an additional factor of T/T_1. Ballistic disorder leads to corrections to both rates that are proportional to T and always small compared to the clean contribution.[28,29] As explained in the Appendix, the arguments given in Sec. II C 3 give the correct temperature scaling of the disorder corrections, but not the correct sign.

The interband contribution is exponentially small at asymptotically low temperatures, and therefore was not considered in Ref. 30. However, for values of the pitch wave number that are not too small it may dominate in a temperature window, as we now show. Using Eq. (2.11) instead of (2.10) we obtain for the single-particle rate due to interband scattering

$$\frac{1}{\tau_{\rm sp}} \propto \lambda\,\frac{q}{k_{\rm F}}\left(\frac{T}{T_1}\right)^{1/2}\int_{T_0/T}^{T_1/T}\frac{dx}{\sqrt{x}}\int_0^\infty dz\,\frac{1}{\sqrt{z^2+x^2}} \times\frac{1}{\sinh\sqrt{z^2+x^2}}. \tag{3.8a}$$

The dimensionless integral provides an additional factor of $\sqrt{T/T_0}$, and we obtain

$$\frac{1}{\tau_{\rm sp}}\propto\lambda\,\frac{q}{k_{\rm F}}\times\begin{cases}\sqrt{T/T_1}\,e^{-T_0/T} & \text{for} \quad T\lesssim T_0\\ T/\sqrt{T_0T_1} & \text{for} \quad T_0\lesssim T\lesssim T_q\end{cases}. \tag{3.8b}$$

In the case of the transport rate the backscattering factor renders the dimensionless integral a constant, and we find

$$\frac{1}{\tau_{\rm tr}}\propto\lambda\left(\frac{q}{k_{\rm F}}\right)^4\left(\frac{T}{T_q}\right)^{3/2}\times\begin{cases}e^{-T_0/T} & \text{for} \quad T\lesssim T_0\\ 1 & \text{for} \quad T_0\lesssim T\lesssim T_q\end{cases}. \tag{3.9}$$

For the electrical resistivity, this implies Eq. (1.4). These results are valid for $T\lesssim T_q=Dq^2$; for higher temperatures they cross over to the FM results. The temperature window where the resistivity scales as $T^{3/2}$ thus may or may not exist, depending on the value of the ratio $\epsilon_{\rm F}q/\lambda k_{\rm F}$.

As an alternative to the above derivation one can repeat the HM calculation of Ref. 30 or 29 and take into account the interband scattering terms that were neglected in these references. The result is the same. We also note that, while the resistivity in a HM is anisotropic, the two independent components of the resistivity tensor differ only by a numerical factor.[29]

In the presence of disorder the dimensionless integral is only logarithmically divergent in the infrared, rather than power-law divergent as in Eq. (3.8a). At the same time, the lower cutoff T_0/T disappears and is replaced by T_L/T, where $T_L = D/L^2$ with L the linear system size. We then obtain a disorder correction to the rates, to leading logarithmic accuracy,

$$\delta(1/\tau_{\rm sp}) \propto \delta(1/\tau_{\rm tr}) \;\propto\; \frac{1}{\tau}\left(\frac{q}{k_{\rm F}}\right)^3 \frac{\epsilon_{\rm F}}{\lambda}\,\frac{T}{T_q}\,\ln(T/T_L) \qquad (T_{\rm ball} \lesssim T \lesssim T_q)\;. \tag{3.10}$$

This may or may not dominate over the clean contribution, depending on the parameter values. We note, however, that this result, and in particular its remarkable logarithmic dependence on the system size, depend on the convergence properties of the dimensional integral. A more detailed investigation of where the power-law divergence crosses over to a logarithmic one is therefore warranted in order to determine the range of validity and the prefactor of the $T \ln T$ behavior.[42] However, any such analysis will be highly model dependent, and for the purposes of the current general discussion we therefore defer to a future investigation.

IV. SUMMARY, AND DISCUSSION

Before we give a discussion of our results, we present a summary in the form of Table I. It lists the three process we have identified that lead to a $T^{3/2}$ behavior of the electrical resistivity, as well as the other seven scattering processes we have discussed, and also summarizes our results for the thermal resistivity.

We now discuss various aspects of our results. We first make some purely theoretical remarks, and then discuss issues relevant for comparing with experiments.

A. Theoretical remarks

Let us make contact with previous theoretical work on columnar fluctuations in Refs. 44 and 25. In order to relate to the former, we note that the wave-number-resolved quasiparticle rate, which is given by Eq. (2.10) or (2.11) without the sum over $\boldsymbol{k}$, for special directions of $\boldsymbol{k}$, scales asymptotically as $T^{5/4}$ in clean systems, with a disorder correction that scales as T. This behavior does not show in the rate that determines the thermal resistivity, which gets averaged over the Fermi surface. Similarly, a wave-number-resolved "transport rate" (i.e., the wave-number-resolved single-particle rate with an additional momentum squared in the integrand) scales asymptotically as $T^{7/4}$ in clean systems, in agreement with Ref. 44. Again, this behavior does not show in the electrical resistivity, which is determined by the true transport rate that involves an average over the Fermi surface. Reference 25 considered intraband scattering due to columnar fluctuations in general, and pointed out that in conjunction with ballistic disorder they lead to a $T^{3/2}$ contribution to the resistivity. While this is generally valid, the particular realization of columnar fluctuations in terms of a superposition of helices proposed for MnSi in Ref. 26 leads to a contribution that is negative and always small compared to the clean T^3 contribution, see Sec. III B and Table I. By contrast, the corresponding interband scattering process considered in Sec. III B comes with a positive prefactor that is much larger, and thus a better candidate for explaining the observations in MnSi. We will give a more detailed comparison with experimental observations in Sec. IV B.

The last remark raises the question of why ballistic disorder does not always just lead to a small correction to the clean scattering rate. The answer is that in general it does. However, interband scattering provides a way to avoid this conclusion: Since the clean rate is exponentially small for $T \lesssim T_0$, and since disorder eliminates the energy threshold that leads to this suppression, the disorder "correction" is actually the leading term in the temperature region $T_{\rm ball} \lesssim T \lesssim T_0$.

We note that in Dzyaloshinksii-Moriya helimagnets, the helimagnon scattering mechanisms are always suppressed compared to the skyrmion mechanism, or the FM mechanism at larger wave numbers, due to the small value of $q/k_{\rm F}$, which in turn is a consequence of the small spin-orbit coupling. This would be different in systems with a modulated spin order whose wave number is not small compared to $k_{\rm F}$. In this context we mention that our general expressions (2.10, 2.11), do apply to antiferromagnets. In this case $q \approx k_{\rm F}$, the resonance frequency is linear in k, and the relevant susceptibility is given by the same expression as for HMs, Eq. (2.4b). However, antiferromagnetic magnons are not soft enough to lead to NFL effects. It is interesting to note, though, that electronic stripe phases have Goldstone modes that have the same form as in HMs, but with much larger values of q.[45] Such systems would therefore be of interest to investigate systematically with respect to transport anomalies.

An important aspect of Eqs. (2.10) and (2.11) is that the rate for interband scattering is lacking the gradient-squared factor that is present in the intraband expression. The reason is that electrons within a given subband cannot couple directly to the phase of the magnetic order parameter, since that phase has no physical significance. Rather, the coupling is to the gradient of the phase. For electrons within two different subbands, on the other hand, the coupling is to a phase difference, which does have a physical meaning. This was noted before in Ref. 36 in the context of FMs. It is equally important for the HM cases discussed here, and it is the reason why the clean interband scattering rates have a stronger temperature dependence than the intraband ones, see Table I.

It may not be obvious why the phase susceptibility in the skyrmionic case, Eq. (2.4c), has qualitatively differ-

Table I: Summary of temperature dependences of the single-particle scattering rate, or the thermal resistivity contribution $\delta\rho_{\rm th}$, and the transport rate, or the electrical resistivity contribution $\delta\rho_{\rm el}$, for different magnets and scattering mechanisms with or without ballistic disorder. Also shown is the prefactor $A_{3/2}$ for the electrical resistivity, $\delta\rho_{\rm el}(T) = A_{3/2}T^{3/2}$, if applicable. $\rho_0 = m_e/ne^2\tau$ is the residual resistivity, and $\rho_\lambda = m_e\lambda/ne^2$. See the text for additional information.

System	Soft Modes	Scattering	Ballistic Disorder	Single-particle Rate / $\delta\rho_{\rm th}$	Transport Rate / $\delta\rho_{\rm el}$	Prefactor $A_{3/2}$	References
FM	magnons	interband	No [a]	$T\ln(T_0/T)$	T^2		36,43
			Yes [b]	$T^{3/2}$	$T^{3/2}$	$\rho_0/T_1T_0^{1/2}$	This work
		intraband			N/A		
HM	skyrmions	interband	No [a),c]	$T\ln^2(T/T_0)\to T$	$T^2\to T^{3/2}$		This work
			Yes [b),c]	$T^{3/2}\to T^{5/4}$	$T^{3/2}\to T^{5/4}$	$\rho_0/T_1T_0^{1/2}$	This work
		intraband	No [c]	$T^2\to T^{3/2}$	$T^3\to T^2$		This work
			Yes [d]	$(T^{3/2}\to T^{5/4})$	$(T^{3/2}\to T^{5/4})$		This work, 25
HM	helimagnons	interband	No [a]	T [e]	$T^{3/2}$	$\rho_\lambda(q/k_{\rm F})/T_1^{3/2}$	This work
			Yes [b]	$T\ln(T/T_L)$	$T\ln(T/T_L)$		This work
		intraband [f]	No	$T^{3/2}$	$T^{5/2}$		30
			Yes [g]	(T)	(T)		28,29

[a] Valid for $T \gtrsim T_0$; crossover to exponentially small rates for lower T due to exchange gap.
[b] Valid for $T \gg T_{\rm ball}$; crossover to diffusive dynamics for lower T.
[c] Arrows indicate crossover at asymptotically low T due to different dynamics, see Ref. 35 and the discussion in Sec. III B.
[d] Corrections to rates due to ballistic disorder are negative and always small compared to the clean contributions.
[e] This should properly be interpreted as $T^{1/2}\times T^{1/2}$, as explained in the text.
[f] Valid for systems on a cubic lattice.
[g] Corrections to rates due to ballistic disorder are positive and always small compared to the clean contributions.

ent forms in the preasymptotic and asymptotic regions, respectively. The reason is that the static susceptibility, $\chi(\boldsymbol{k}) = \int(d\omega/\pi){\rm Im}\,\chi(\boldsymbol{k}, i\Omega\to\omega+i0)$, must be equal to the Goldstone mode in both regimes. The latter is known from Ref. 34, and the requirement that both the preasymptotic resonance frequency, Eq. (2.3b), and the asymptotic one, Eq. (2.3c), yield the same result for the static suscepbility dictates the form of $\chi(\boldsymbol{k}, i\Omega)$ in the second line in Eq. (2.4c).

We finally give an argument for the 3/2 exponent in the FM case to be exact, rather than a perturbative result that could change at higher orders in the effective interaction. Consider Eq. (3.2) in Ref. 46, which gives a general homogeneity law for the scaling part of the electrical conductivity of a FM. Ballistic disorder eliminates the backscattering factor that enters the scale dimension of the conductivity, so in our present context the latter is equal to $(d-2)-2(d-1) = -d$ instead of $(d-4)-2(d-1) = -(d+2)$. The relevant dynamical exponent for magnon scattering is $z = 2$, which leads to $T^{-3/2}$ for the scaling part of σ in $d = 3$, or $T^{3/2}$ for the scaling part of ρ.

B. Comparison with experiments

In order to compare our results with experiments, we first need to keep in mind that we ignored all numerical prefactors, which in any case are model dependent. We therefore can aim only for very rough, order-of-magnitude comparisons with experimental results.

We start by discussing the energy scales defined in Sec. II B for low-temperature magnets such as MnSi, $ZrZn_2$, or Ni_3Al. The spin-stiffness coefficient is directly measurable, and typically on the order of $D \approx 25 - 50\,{\rm meV\,\AA^2}$.[47,48] For T_1 this implies values on the order of 100s of K. The pitch wave number in helimagnets is directly measurable. In MnSi, $q \approx 0.035{\rm \AA}^{-1}$.[49] This implies that T_q is on the order of 100s of mK. For reasonably clean materials ($\rho_0 \lesssim 1\mu\Omega{\rm cm}$), the mean-free path is large compared to any reasonable value atomic scale, so $T_{\rm ball}$ will me on the order of 1 mK or less, and can be ignored in the context of all existing experimental results. This leaves the value of T_0, which depends on the ratio $\lambda/\epsilon_{\rm F}$, which is much harder to determine. From band structure calculations, λ is typically on the order of thousands of K.[50–52] This is consistent with Stoner theory, where $\lambda = 6T_1$, although λ can be highly anisotropic

in wave-number space.[52] If one takes $\lambda = 5,000$K, and $\epsilon_F = 10^5 K$, a typical value for a simple good metal, then one has $\lambda/\epsilon_F \approx 0.05$ at most, or $T_0 \approx 1$K. However, this is likely misleading for most real materials. The band structures of low-temperature ferromagnets are fairly complicated, and the exchange splitting has been suggested to be as large as 0.4 times the relevant effective Fermi energy.[53] This suggests values of T_0 on the order of 10s of K. Based on this discussion, we conclude that reasonable effective values are, very roughly, $T_{\rm ball} \approx 1$mK, $T_q \approx 250$mK, $T_0 \approx 10$K, $T_1 \approx 250$K, $\lambda/\epsilon_F \approx 0.1$, and $q/k_F \approx 0.03$, with T_0 the most uncertain.

Given these estimates, the range of validity of Mechanisms 1 and 2 is the same as the temperature range for which a $T^{3/2}$ behavior, or something close to it, is observed in $ZrZn_2$ and other low-temperature FMs, and in the disordered phase of the HM MnSi, viz., a few mK to several K. Let us now consider the prefactor of the $T^{3/2}$ law

$$\delta\rho(T) = A_{3/2} T^{3/2} \ . \tag{4.1}$$

If we ignore all numerical prefactors, as we did in Sec. III, we obtain Eqs. (1.2) and (1.3) with $\gamma_1 = \gamma_2 = 1$. With the temperature scales as estimated above, this yields $A_{3/2} \approx 0.001 \mu\Omega$cm/K$^{3/2}$, which is a factor of 10 smaller than what is observed in $ZrZn_2$, and a factor of 100 smaller than what is observed in MnSi. If we take the numerical factors seriously, we have, after various cancellations, a factor of π from the spectrum of the susceptibility, and a factor of about 3 from the dimensional integral in Eq. (3.3a), or a factor of about 6 from the one that enters Eq. (3.5). This leads to $\gamma_1 \approx 10$, and $\gamma_2 \approx 20$. While these estimates should not be taken too seriously, they indicate that Mechanism 1 produces a prefactor $A_{3/2}$ that is very close to what is observed in $ZrZn_2$, and Mechanism 2 produces a $A_{3/2}$ that is within a factor of 5 of what is observed in the disordered phase of MnSi. For the latter, we assume that columnar fluctuations exist in this phase, as was proposed in Ref. 25. There is strong experimental evidence,[15] as well as theoretical arguments,[16] for this phase to be a strongly correlated liquid-like phase. The associated strong fluctuations are expected to enhance the prefactor compared to our simple relaxation-rate considerations and may well account for the remaining factor of 5.

Let us now briefly discuss the ordered phase of MnSi, where the observed resistivity behavior is T^2, see Fig. 2. In this context it is important to remember that there are many contributions to the electron scattering rate, e.g., due to the Coulomb interaction, phonons, and other excitations, that lead to contributions that go as T^s with $s \geq 2$. We have focused on the contributions due to magnetic Goldstone modes, which have the remarkable property that they lead to a $T^{3/2}$ behavior. In addition to whatever scattering mechanism is producing the T^2 behavior in the helically ordered phase of MnSi, we therefore expect a $T^{3/2}$ contribution for $T > T_q$, where MnSi effectively behaves like a FM and Mechanism 1 applies, and a $T \ln T$ contribution for $T < T_q$, where Eq. (3.10) applies (note, however, the caveats mentioned after Eq. (3.10), which requires a thorougher investigation). Consider the former regime, and write the resistivity as

$$\delta\rho = A_{3/2} T^{3/2} + A_2 T^2 \quad (T \gtrsim T_q) \ . \tag{4.2a}$$

For A_2 we take the observed value $A_2 \approx 0.03 \mu\Omega$cm/K^2.[14] For $A_{3/2}$ we expect a value comparable to that observed in $ZrZn_2$ and other low-temperature FMs, $A_{3/2} \approx 0.01 \mu\Omega$cm/K$^{3/2}$. The $T^{3/2}$ term will then dominate for $T \lesssim (A_{3/2}/A_2)^2 \approx 100$mK, which is less than T_q. The $T^{3/2}$ contribution will therefore be a small correction to the dominant T^2 behavior at all temperature where Eq. (3.3b), or equivalently Eq. (1.2), applies to MnSi. In the latter regime, the helical nature of the Goldstone modes will be apparent, and various nonanalytic contributions to $\delta\rho$ must be present. The $T^{5/2}$ contribution from clean intraband HM scattering is too weak to be observable, and the disorder contribution due to interband scattering comes with the caveats mentioned after Eq. (3.10) and requires a more detailed investigation. Ignoring these caveats, and ignoring the logarithm, we expect

$$\delta\rho = A_1 T + A_2 T^2 \quad (T \lesssim T_q) \ . \tag{4.2b}$$

With the same parameters as used above one finds $A_1 \approx 10^{-3} \mu\Omega$cm/K. The $T \ln T$ term will thus dominate over the T^2 term only for temperatures small compared to about 30mK, although the logarithm, and a more thorough determination of the prefactor, might change this estimate. We conclude that any nonanalytic contribution to $\delta\rho$ in the helically ordered phase would require a precision experiment at temperatures smaller than at least 100mK.

The T^s behavior with $1.5 \lesssim s < 2$ observed in $ZrZn_2$ is most likely the result of a $T^{3/2}$ behavior due to Mechanism 1 in addition to a T^2 contribution from other scattering mechanisms. If one takes Eq. (4.2a) with $A_{3/2}/A_2 \approx 1$K$^{1/2}$, then between about 100mK and 10K the behavior is well represented by a single $T^{1.7}$ law. Another question is why the transport anomaly is observed in the magnetically disordered phase as well as in the ordered one. A plausible answer lies in the fact that the magnetic transition is first order. As has been discussed in Ref. 31, even very weak quenched disorder leads to static islands or droplets of the ordered phase within the disordered one, which explains the commonly observed phase separation in the vicinity of first-order transitions (see Refs. 22–24 for examples). It also explains why the Goldstone modes of the ordered phase, i.e., the FM magnons, can still contribute to the scattering of electrons even in the magnetically disordered phase.

We have focused on MnSi and $ZrZn_2$ in this discussion since these are the experimentally best studied systems. There are, however, many other examples of low-temperature ferromagnets where NFL behavior has been

observed: Off-stoichiometric $NiGa_3$ is a FM for Ni-rich concentrations and displays a NFL $T^{3/2}$ behavior with a coefficient of $A_{3/2} \approx 0.04\mu\Omega\text{cm/K}^{3/2}$.[14,18] For smaller Ni concentrations the material is paramagnetic and $\delta\rho$ is Fermi-liquid-like. The stoichiometric compound has the smallest residual resistivity, $\rho_0 \approx 1\mu\Omega$cm. In Ni_3Al under pressure, for samples with $\rho_0 \approx 1\mu\Omega$cm, a $T^{3/2}$ dependence, or a power law close to that, is observed on either side of the ferromagnetic transition with a coefficient $A_{3/2} \approx 0.02\mu\Omega\text{cm/K}^{3/2}$, see Ref. 8. Similar observations in more disordered systems include $Nb_{1-x}Fe_{2+x}$, for which a $T^{3/2}$ behavior has been observed on the non-magnetic side of a magnetic transition.[17] In this case, $\rho_0 \approx 5\mu\Omega$cm. In $(Ni_{1-x}Pd_x)_3Al$, with $\rho_0 \approx 10\mu\Omega$cm, a $T^{3/2}$ behavior was found on both sides of the FM transition.[7] All of these observations can be understood at a semi-quantitative level by a discussion analogous to the one given above, which slightly different parameter values.

Finally, our results suggest a number of possible experiments. One interesting question is whether or not there is a small NFL contribution to the resistivity in the ordered phase of MnSi. As discussed above, this would require a precise determination of the resistivity at very low temperatures, probably lower than 100mK. This would entail subtracting the T^2 contribution to reveal any underlying NFL behavior. Of particular interest is the logarithmic dependence on the sample size predicted by Eq. (3.10). It suggests that, in systems small enough for the spin-orbit coupling not to intervene, the resistivity (*not* just the resistance) will change with changing sample size, which reflects the soft helimagnon excitations in a HM phase. Additional theoretical investigations are also called for to make this prediction more precise.[42] Another interesting question is the magnetic-field dependence of the NFL resistivity. For the FM mechanism, Eq. (1.2), the theory predicts that in a field H such that $\mu_B H > T$ the magnon-induced resistivity contribution becomes $\delta\rho_{\text{FM}} \propto T^2/H^{1/2}$. A study of the magnetoresistance of $ZrZn_2$ would be very interesting in that respect.

Acknowledgments

This work was supported by the NSF under Grant Nos. DMR-1401449 and DMR-1401410. This work was initiated at the Aspen Center for Physics, supported by the NSF under Grant No. PHYS-1066293, and continued at the Telluride Science Research Center (TSRC).

Appendix: Disordered helimagnets in the ballistic limit

In this appendix we discuss the relation between the simple arguments given in Sec. II C 3 about the effects of disorder in the ballistic regime and a detailed calculation. This also sheds light on the confusing issue of the sign of the disorder correction to the relaxation rates, which is different for the case of helimagnon interband scattering from all of the other cases.

To make the salient point it suffices to consider the single-particle rate, which is given as the imaginary part of the electronic self energy. In the presence of weak disorder, the leading correction to the clean result is given by the diagram shown in Fig. 5. Analytically, this contribution is (see Eq. (3.11) in Ref. 29)

$$\frac{1}{\tau_{\text{sp}}} \propto \frac{1}{\tau}\,\frac{D\epsilon_{\text{F}}^2 q^2}{N_{\text{F}}}\,\frac{1}{V}\sum_{\boldsymbol{k}} \text{Im}L^{++,-}(\boldsymbol{k}) \times \int_{-\infty}^{\infty}\frac{du}{\pi}\, n_{\text{F}}(u/T)\,\chi''(\boldsymbol{k},u)\ . \tag{A.1a}$$

Here $n_{\text{F}} = 1/(e^x+1)$ is the Fermi distribution function, and

$$L^{++,-}(\boldsymbol{k}) = \frac{1}{V}\sum_{\boldsymbol{p}} \gamma(\boldsymbol{k},\boldsymbol{p})\,\gamma(\boldsymbol{k},\boldsymbol{p}-\boldsymbol{k})\ G_R^2(\boldsymbol{p})\,G_A(\boldsymbol{p}-\boldsymbol{k})\ , \tag{A.1b}$$

and we have kept only terms that contribute to the leading temperature dependence of $1/\tau_{\text{sp}}$. G_R and G_A are the retarded and advanced Green function, respectively. In the case of intraband scattering all three Green functions belong to the same Fermi surface. The couplings γ depend in general on both the transferred momentum and the momentum of the incoming or outgoing electron. In the case of interband scattering, they are constants. In the case of interband scattering, they are gradients that in Eq. (2.11) we have represented by the transferred momentum, $\gamma(\boldsymbol{k},\boldsymbol{p}) \propto \boldsymbol{k}$. This is qualitatively correct in the case of skyrmionic fluctuations, where k_z provides the leading temperature scaling, see Eqs. (2.3), and the angular part of the integral in Eq. (A.1a) is

$$\int_{-1}^{1} d\eta\ \frac{1}{(v_{\text{F}}k\eta - i0)^2} = \frac{-2}{(v_{\text{F}}k)^2}\ . \tag{A.2a}$$

However, in the case of helimagnon scattering, where the leading scaling is provided by $\boldsymbol{k}_\perp$, the dependence of γ on $\boldsymbol{k}_\perp$ comes in the form $(\boldsymbol{k}_\perp\cdot\boldsymbol{p}_\perp)p_z$, see Eq. (2.18c) in Ref. 28. This introduces an angular dependence of the integrand that is not present in the schematic representation in Eq. (2.11). The relevant angular integral then is

$$\int_0^{2\pi} d\varphi\ \frac{\cos^2\varphi}{(v_{\text{F}}k_\perp\cos\varphi - i0)^2} = \frac{1}{(v_{\text{F}}k_\perp)^2}\ . \tag{A.2b}$$

The sign of the disorder correction is thus different in the two cases. For the case of helimagnon interband scattering, where Eq. (A.2b) applies, we recover the result of Ref. 28, viz.

$$\delta\,(1/\tau_{\text{sp}}) \propto \frac{1}{\tau}\left(\frac{q}{k_{\text{F}}}\right)^5 \frac{\epsilon_{\text{F}}}{\lambda}\left[\frac{-\Lambda}{T_q} + \ln 2\,\frac{T}{T_q}\right]\ . \tag{A.3}$$

Here Λ is a UV energy cutoff. The cutoff-dependent constant contribution to the rate is negative, so the effect is

antilocalizing, and the universal temperature-dependent contribution is accordingly positive. For the interband skyrmion case, on the other hand, Eq. (A.2a) applies. The effect then has the opposite sign and is localizing, i.e., the temperature-dependent disorder correction to the rate is negative.

Now compare these results with the simple argument given in Sec. II C 3, which replaces $\mathrm{Im}L^{++,-}(\boldsymbol{k})$ with

$$L(\boldsymbol{k}) = \int_{-1}^{1} d\eta \, \frac{1/\tau}{(v_{\mathrm{F}}k\eta)^2 + 1/\tau^2} = \frac{1}{v_{\mathrm{F}}k}\left[\frac{\pi}{2} - \frac{1}{v_{\mathrm{F}}k\tau} + \ldots\right] . \tag{A.4}$$

The simple argument thus yields the correct momentum or temperature scaling in both cases, but produces the wrong sign in the helimagnon case.

Finally, consider the case of interband scattering, where G_R belong to one subband, and G_A to the other. The relevant angular integral then is

$$\int_{-1}^{1} d\eta \, \frac{1}{(v_{\mathrm{F}}k\eta - 2\lambda - i0)^2} = \frac{1}{2\lambda^2} \tag{A.5a}$$

for $k \to 0$. The simple smearing argument replaces this by

$$\int_{-1}^{1} d\eta \, \frac{1}{(v_{\mathrm{F}}k\eta - 2\lambda)^2 + 1/\tau^2} = \frac{1}{2\lambda^2} \qquad (v_{\mathrm{F}}k \ll \lambda \ , \ \lambda \gg 1/\tau) \ , \tag{A.5b}$$

and thus produces the correct result.

In conclusion, the simple δ-function smearing argument from Sec. II C 3 yields the correct temperature scaling for all of the cases considered, and the correct sign of the disorder correction except in the case of intraband helimagnon scattering.

[1] A. A. Abrikosov, L. P. Gorkov, and I. E. Dzyaloshinski, *Methods of Quantum Field Theory in Statistical Physics* (Dover, New York, 1963).
[2] A. H. Wilson, *The Theory of Metals* (Cambridge University Press, Cambridge, 1954).
[3] C. Kittel, *Introduction to Solid State Physics* (Wiley, New York, 2005).
[4] J. Hertz, Phys. Rev. B **14**, 1165 (1976).
[5] A. J. Millis, Phys. Rev. B **48**, 7183 (1993).
[6] S. Takashima, M. Nohara, H. Ueda, N. Takeshita, C. Terakura, F. Sakai, and H. Takagi, J. Phys. Soc. Jpn. **76**, 043704 (2007).
[7] M. Sato, J. Phys. Soc. Japan **39**, 187004 (1975).
[8] P. G. Niklowitz, F. Beckers, G. G. Lonzarich, G. Knebel, B. Salce, J. Thomasson, N. Bernhoeft, D. Braithwaite, and J. Flouquet, Phys. Rev. B **72**, 024424 (2005).
[9] P. Khalifah, I. Ohkubo, H. M. Christen, and D. G. Mandrus, Phys. Rev. B **70**, 134426 (2004).
[10] C. Pfleiderer, S. R. Julian, and G. G. Lonzarich, Nature (London) **414**, 427 (2001).
[11] P. A. Lee and T. V. Ramakrishnan, Rev. Mod. Phys. **57**, 287 (1985).
[12] D. Belitz and T. R. Kirkpatrick, Rev. Mod. Phys. **66**, 261 (1994).
[13] C. Pfleiderer, G. J. McMullan, S. R. Julian, and G. G. Lonzarich, Phys. Rev. B **55**, 8330 (1997).
[14] C. Pfleiderer, J. Low Temp. Phys. **147**, 231 (2007).
[15] C. Pfleiderer, D. Reznik, L. Pintschovius, H. v. Löhneysen, M. Garst, and A. Rosch, Nature (London) **427**, 227 (2004).
[16] S. Tewari, D. Belitz, and T. R. Kirkpatrick, Phys. Rev. Lett. **96**, 047207 (2006).
[17] M. Brando, W. J. Duncan, D. Moroni-Klementowicz, C. Albrecht, D. Gruner, R. Ballou, and F. M. Grosche, Phys. Rev. Lett. **101**, 026401 (2008).
[18] J. H. J. Fluitman, R. Boom, P. F. De Chatel, C. J. Schinkel, J. L. L. Tilanus, and B. R. de Vries, J. Phys. F **3**, 109 (1973).
[19] D. Belitz, T. R. Kirkpatrick, and T. Vojta, Phys. Rev. Lett. **82**, 4707 (1999).
[20] T. R. Kirkpatrick and D. Belitz, Phys. Rev. B **85**, 134451 (2012).
[21] M. Brando, D. Belitz, F. M. Grosche, and T. R. Kirkpatrick, Rev. Mod. Phys. **88**, 025006 (2016).
[22] Y. J. Uemura, T. Goko, I. M. Gat-Maleruanu, J. P. Carlo, P. L. Russo, A. T. Savici, A. Aczel, G. J. MacDougall, J. A. Rodriguez, G. M. Luke, et al., Nature Physics **3**, 29 (2007).
[23] C. Pfleiderer, P. Böni, C. Franz, T. Keller, A. Neugebauer, P. G. Niklowitz, P. Schmakat, M. Schulz, Y. K. Huang, J. A. Mydosh, et al., J. Low Temp. Phys. **161**, 167 (2010).
[24] I. M. Gat-Maleruanu, J. P. Carlo, T. Goko, A. Fukaya, T. Ito, P. P. Kyriakou, M. I. Larkin, G. M. Luke, P. L. Russo, A. T. Savici, et al., Phys. Rev. B **84**, 224415 (2011).
[25] T. R. Kirkpatrick and D. Belitz, Phys. Rev. Lett. **104**, 256404 (2010).
[26] S. Mühlbauer, B. Binz, F. Jonietz, C. Pfleiderer, A. Rosch, A. Neubauer, R. Georgii, and P. Böni, Science **323**, 915 (2009).
[27] G. Zala, B. N. Narozhny, and I. L. Aleiner, Phys. Rev. B **64**, 214204 (2001).
[28] T. R. Kirkpatrick, D. Belitz, and R. Saha, Phys. Rev. B **78**, 094407 (2008), The published version of this paper contains several sign errors, but the final result for the single-particle rate with disorder has the correct sign. See arXiv:0806.0614 for a corrected version.
[29] T. R. Kirkpatrick, D. Belitz, and R. Saha, Phys. Rev. B **78**, 094408 (2008).
[30] D. Belitz, T. R. Kirkpatrick, and A. Rosch, Phys. Rev. B **74**, 024409 (2006).
[31] T. R. Kirkpatrick and D. Belitz, Phys. Rev. B **93**, 144203 (2016).
[32] D. Belitz, T. R. Kirkpatrick, and A. Rosch, Phys. Rev. B **73**, 054431 (2006).
[33] P. G. DeGennes and J. Prost, *The Physics of Liquid Crys-*

tals (Clarendon, Oxford, 1993).
[34] K. Ho, T. R. Kirkpatrick, Y. Sang, and D. Belitz, Phys. Rev. B **82**, 134427 (2010).
[35] O. Petrova and O. Tchernyshyov, Phys. Rev. B **84**, 214433 (2011).
[36] S. Bharadwaj, D. Belitz, and T. R. Kirkpatrick, Phys. Rev. B **89**, 134401 (2014).
[37] Depending on the material, the microscopic energy scale could be a band width rather than the Fermi energy.
[38] In many model calculations T_1 and λ differ only by a factor of $O(1)$. For instance, in a Stoner model one has $\lambda = 6T_1$. However, the two scales are reallly physically distinct. For instance, in bulk metallic ferromagnets the spin-stiffness coefficient has a magnetization dependence $D \propto m_0 \ln(k_F^3/m_0)$,[54] so T_1 is not simply proportional to λ.
[39] This is a schematic representation of the gradient coupling, the actual form is more complicated and depends on the shape of the Fermi surface. For helimagnon scattering in particular, the leading scaling behavior is not realized for a spherical Fermi surface but rather requires a lattice, and the gradient coupling involves an angular dependence that is important for the sign of disorder corrections to $1/\tau_{sp}$; see Refs. 32 and 28, and also Sec. IV and the Appendix.
[40] G. D. Mahan, *Many-Particle Physics* (Plenum, New York, 1981).
[41] D. Belitz and T. R. Kirkpatrick, Physica E **42**, 497 (2010).
[42] Such an analysis will also have to consider terms of higher order in the spin-orbit interaction, which change the dispersion relation of the Goldstone modes at very small wave numbers,[32,34] and replace the dependence on the sample size by a dependence on a spin-orbit related length scale.
[43] K. Ueda and T. Moriya, J. Phys. Soc. Japan **39**, 605 (1975).
[44] H. Watanabe, S. A. Parameswaran, S. Raghu, and A. Vishwanath, Phys. Rev. B **90**, 045145 (2014).
[45] T. R. Kirkpatrick and D. Belitz, Phys. Rev. B **80**, 075121 (2009).
[46] T. R. Kirkpatrick and D. Belitz, Phys. Rev. B **91**, 214407 (2015).
[47] P. Böni, B. Roessli, and K. Hradil, J. Phys. Cond. Matt. **23**, 254209 (2011).
[48] N. R. Bernhoeft, I. Cole, G. G. Lonzarich, and G. L. Squires, J. Appl. Phys. **53**, 8204 (1982).
[49] Y. Ishikawa, K. Tajima, D. Bloch, and M. Roth, Solid State Commun. **19**, 525 (1976).
[50] T. Jeong and W. E. Picket, Phys. Rev. B **70**, 075114 (2004).
[51] D. J. Singh and I. I. Mazin, Phys. Rev. Lett. **88**, 98 (2002).
[52] I. I. Mazin, D. J. Singh, and A. Aguayo, in *Physics of Spin in Solids: Materials, Methods, and Applications*, edited by S. Halilov (Kluwer, New York, 2004), p. 139.
[53] T. I. Sigfusson, N. R. Bernhoeft, and G. G. Lonzarich, J. Phys. F **14**, 2141 (1984).
[54] D. Belitz, T. R. Kirkpatrick, A. J. Millis, and T. Vojta, Phys. Rev. B **58**, 14155 (1998).